INTERNATIONAL JOURNAL OF CLIMATOLOGY
Int. J. Climatol. **30**: 210–219 (2010)
Published online 24 February 2009 in Wiley InterScience
(www.interscience.wiley.com) DOI: 10.1002/joc.1878

RMetS
Royal Meteorological Society

Seasonal prediction of summertime tropical cyclone activity over the East China Sea using the least absolute deviation regression and the Poisson regression

Hyeong-Seog Kim,[a] Chang-Hoi Ho,[a]* Pao-Shin Chu[b] and Joo-Hong Kim[a]
[a] *Climate Physics Laboratory, School of Earth Environmental Sciences, Seoul National University, Seoul, Korea*
[b] *Department of Meteorology, University of Hawaii, Hawaii, USA*

ABSTRACT: In the present study, we have employed two statistical models to predict summertime (July–September) tropical cyclone (TC) activity over the East China Sea using the least absolute deviation (LAD) regression and the Poisson regression method. Through a lagged correlation analysis of the relationship between the seasonal TC frequency in the target region and several pre-season environmental parameters for the period 1979–2003, physically interpretable and statistically significant large-scale environmental parameters were identified as potential predictors. After applying the predictor screening method based on the stepwise regression, three predictors, i.e. sea surface temperature, outgoing long-wave radiation and 850-hPa relative vorticity were finally chosen. They are related to the phase transition of El Niño/Southern Oscillation and the strength of the western North Pacific summer monsoon. The correlation coefficient between the predicted and the observed frequency is 0.75 for the LAD model and 0.78 for the Poisson model. The predictions using the two models have a skill improvement of about 60% compared to the reference forecasts. The present study suggests that both models are skillful in predicting summertime TC frequency over the East China Sea with the Poisson model being slightly more skillful than the LAD model. Copyright © 2009 Royal Meteorological Society

KEY WORDS East China Sea; tropical cyclone; seasonal prediction; statistical prediction; least absolute deviation regression; Poisson regression

Received 15 February 2008; Revised 17 November 2008; Accepted 21 January 2009

1. Introduction

Tropical cyclone (TC) is one of the most devastating natural phenomena seen in East Asia. Every year, during peak TC season (July–September), East Asian people living in coastal areas suffer serious social and economic damage from the strong winds and torrential rain induced by land-falling TCs. To reduce the damage, it is crucial for weather forecasters to have enhanced capability of real-time forecast on the landfall or approach of TCs to East Asian countries (e.g. China, Japan, Taiwan and Korea). In addition, advanced prediction of seasonal TC frequency in a regional domain would be helpful for decision makers to be more proactive. So to speak, improving our ability of both real-time forecast and seasonal prediction are inevitable to mitigate the potential damage caused by TC-induced prospective flash floods, tidal waves and high winds.

For the prediction of seasonal TC activity, empirical statistical methods that use environmental predictors have been widely applied as a primary operational technique. Gray *et al*. (1992, 1993, 1994) proposed a linear regression model to predict seasonal hurricane activity in the North Atlantic using various preseason environmental parameters, such as El Niño/Southern Oscillation (ENSO), Quasi-Biennial Oscillation and western Sahel rainfall. Elsner and Schmertmann (1993) developed a skillful seasonal prediction method for intense hurricanes using a nonlinear Poisson regression model. Further, Hess *et al*. (1995) improved the hurricane forecasting by separating tropical-only hurricanes from those influenced by extra-tropical factors. On the other hand, the prediction of seasonal TC frequency in the western North Pacific (WNP) was pioneered by Chan *et al*. (1998, 2001). They developed a seasonal prediction model using a projection pursuit regression technique, which incorporates various preseason environmental parameters, including ENSO, cold surge, polar vortex and so on. Recently, Lee *et al*. (2007) attempted to increase the performance of the prediction model for seasonal TC frequency over the WNP using 'smart predictors'. Smart predictors refer to a combination of predictors, yielding the best prediction performance in a hindcast setting. Along the same line as Lee *et al*. (2007), Kwon *et al*. (2007) suggested the statistical ensemble prediction of seasonal TC frequency by considering the uncertainty of a single forecast. Previous studies demonstrated that basin-wide seasonal TC frequency might be predictable several months in advance by incorporating pre-observed large-scale environmental parameters into the

* Correspondence to: Chang-Hoi Ho, Climate Physics Laboratory, School of Earth Environmental Sciences, Seoul National University, 599 Gwanakno, Gwanak-gu, Seoul 151-747, Korea.
E-mail: hoch@cpl.snu.ac.kr

prescribed statistical relations between predictors and the predictand.

In addition to the prediction of basin-wide seasonal TC activity, there has been an increasing demand for the seasonal prediction of regional TC activity, i.e. the number of TCs influencing a specific domain (Liu and Chan, 2003; Saunders and Lea, 2005; Elsner and Jagger, 2006; Chu *et al*., 2007). Compared with the prediction of basin-wide seasonal TC frequency, the prediction for a specific region may be more complicated because the prediction skill is affected, not only by TC genesis but also by TC track. Many previous studies showed that the genesis locations and the tracks of TCs over the WNP are modulated by various large-scale atmospheric and oceanic phenomena, such as ENSO (e.g. Wang and Chan, 2002; Chan and Liu, 2004; Chu, 2004), the Pacific decadal variability (e.g. Matsuura *et al*., 2003; Ho *et al*., 2004), the intra-seasonal oscillation (or Madden-Julian Oscillation) (e.g. Harr and Elsberry, 1995; Nakazawa, 2006; Kim *et al*., 2008), the Antarctic Oscillation (e.g. Ho *et al*., 2005), and the quasi-stationary Rossby wave train in the upper troposphere (e.g. Kim *et al*., 2005b). However, most of the studies mainly dealt with the contemporary relationship between the phenomena and TC activity, so the relationships demonstrated are not appropriate for their prediction.

Recently, Chu *et al*. (2007) have tried to predict the seasonal TC frequency in the vicinity of Taiwan using environmental predictors, e.g. sea surface temperature (SST), sea level pressure, low-level relative vorticity, precipitable water and vertical wind shear. On the basis of their research, the local TC activity may be predictable in advance using classical statistical tools, such as a multivariate least absolute deviation (LAD) regression (Gray *et al*., 1992). Motivated by their studies, we attempt to predict the seasonal TC activity over the East China Sea, where the TCs striking East Asian countries normally pass. We examine the preseason environmental parameters that correlate with the seasonal TC frequency over the target region and found physically reasonable signals of ENSO and the WNP summer monsoon. Using these lag-correlated environmental parameters, we employ statistical prediction models using two regression techniques: the LAD regression and the Poisson regression.

The structure of this paper is as follows. The data and the statistical methods are presented in Section 2. The analyses of large-scale environmental parameters that correlate with summertime TC activity over the East China Sea and the determination of predictors are described in Section 3. The results of the statistical models are discussed in Section 4 and the conclusion is given in Section 5.

2. Data and prediction method

2.1. Data

This study utilizes the dataset of TC activity archived by the Regional Specialized Meteorological Centers-Tokyo Typhoon Center. The dataset contains information about the name, date, TC type, latitude and longitude position, central pressure and maximum sustained wind speed (v_{max}) of TCs at 6-h intervals. In general, TCs are divided into three stages depending on v_{max}: tropical depression ($v_{max} < 17$ m s^{-1}), tropical storm (17 m s^{-1} $\leq v_{max} <$ 34 m s^{-1}) and typhoon ($v_{max} \geq 34$ m s^{-1}). Here, TC refers to tropical storms and typhoons that have a v_{max} greater than 17 m s^{-1}. While the TC data are available from 1951 to the present, there may be reliability problems with the locations and intensities of the TCs in early periods prior to satellite observation. Also, there are inter-decadal changes in the TC tracks associated with the westward expansion of the WNP sub-tropical high in the late 1970s (e.g. Ho *et al*., 2004). Thus, we confine the analysis period to 1979–2007 (29 years) in order to avoid these potential impacts.

Various atmospheric and oceanic data are used to determine the predictors. The sea level pressure, 850-hPa zonal wind and 850-hPa relative vorticity data were obtained from the National Centers for Environmental Prediction-Department of Energy (NCEP-DOE) reanalysis-2 (Kanamitsu *et al*., 2002). The NCEP-DOE reanalysis-2 data have a horizontal resolution of 2.5° × 2.5° in latitude–longitude. The monthly mean SST and outgoing long-wave radiation (OLR) data are taken from the National Oceanic and Atmospheric Administration-Climate Diagnostic Center. The SST and OLR data have a horizontal resolution of 2° × 2° and 2.5° × 2.5° in latitude–longitude, respectively. The available period of these datasets covers the analysis period of this study.

2.2. Statistical prediction method

2.2.1. LAD regression

The multivariate linear regression model is generally presented as

$$\hat{y} = a_0 + \sum_{i=1}^{k} a_i x_i \tag{1}$$

where $\hat{y}$ is the predicted value, a_0 is the regression constant, k is the number of predictors, x_i represents the predictors, and a_i are the corresponding regression coefficients. In the LAD regression, the regression coefficients and constant are obtained by minimizing a sum of absolute errors (SAE) for the training period. The SAE is calculated by the absolute values of the difference between the original values and the predicted values, as follows in Equation (2).

$$\mathrm{SAE} = \sum_{j=1}^{N} |y_j - \hat{y}_j| = \sum_{j=1}^{N} \left| y_j - a_0 - \sum_{i=1}^{k} a_i x_{ij} \right| \tag{2}$$

where N is the training period, y_j are the original values, and the others are the same as in Equation (1).

Because the LAD regression uses the SAE instead of a sum of square errors, which is used in an ordinary least square error regression, the LAD regression is less

sensitive to extreme values and statistically more stable than the least square error regression. The LAD regression is more adequate for small sample size problem because it does not assume that the residuals follow a Gaussian distribution. For these reasons, the LAD regression has been widely used for the statistical models to predict the seasonal TC activity both in the North Atlantic and in the WNP (e.g. Gray *et al*., 1992, 1993, 1994; Chu *et al*., 2007).

The LAD regression cannot be solved in an analytical way because of the absolute operation. For this purpose, we use the Bloomfield-Steiger algorithm (Bloomfield and Steiger, 1980), which is based on the method to solve the linear programming problem using an iteration method. The LAD regression can be converted to the linear programming problem because they are similar in basic nature. The Bloomfield-Steiger algorithm has a concept of finding the normalized steepest direction to minimize the SAE in each iteration process, so that it allows efficient calculation in practice. A detailed explanation and pseudo code for the Bloomfield-Steiger algorithm are given by Chu *et al*. (2007).

2.2.2. *Poisson regression*

The Poisson probability distribution of the number of occurrences of an event is expressed in the following equation.

$$P(h|\lambda) = \frac{e^{-\lambda}\lambda^h}{h!} \text{ for } h = 0, 1, 2, \ldots \text{ and } \lambda > 0 \quad (3)$$

where h denotes the number of occurrences of an event and λ is the Poisson intensity parameter. The Poisson distribution restricts the possible outcomes to non-negative values. This restriction is suitable for the prediction of the number of TC occurrences because it is always represented by a non-negative integer (Elsner and Schmertmann, 1993; McDonell and Holbrook, 2004).

In the Poisson regression model, the expected number of occurrences of the event, i.e. the predictand, is assumed as the exponential function of the linear combinations of the predictors, as seen in the following equation.

$$E[P(h|\lambda)] = \exp\left(\sum_{i=1}^{k} \beta_i x_i + \beta_0\right) \quad (4)$$

where k is the number of predictors, x_i represents the predictors, β_i are the corresponding regression coefficients, and β_0 is the regression constant. The regression coefficients and constant are estimated by maximizing the likelihood of the predictand in Equation (3) using the iteration method.

3. Statistical prediction

3.1. Predictand

The target area of the prediction in this study is 25–35°N and 120–130°E (the box region in Figure 1(a)). The target region covers the East China Sea, including the east coast of China, the south coast of the Korean peninsula and the southwest coast of Japan. The TCs of which centres enter the region at least once during their life time are considered the TC passing through the region. Many TCs, forming in the Philippine Sea, pass across this region, recurve near the latitude 25°N, and then approach the East Asian centuries (Figure 1(a)). Among the 114 TCs passing through the region during July–September, 94 TCs (82% of the total TCs) strike either the China, Taiwan, Korea or Japan. Figure 1(b) depicts the climatological distribution of the monthly TC frequency passing across the target region, showing a large seasonal variation. The climatological number of TCs is about one for July and September, about 1.6 for August, about 0.5 for June and October, less than 0.1 for April, May, and November, and none for December to March. The number of summertime (July–September) TCs is equivalent to about 75% of the annual number of TCs passing over the East China Sea. Most of the damage caused by TCs in East Asia occurs during these 3 months. For this reason, we confine the prediction season to July, August and September.

3.2. Potential predictors

To examine the precursory effects of large-scale environments, we perform a lagged correlation analysis of the relationship between the frequency of the summertime TCs passing over the East China Sea (i.e. predictand) and the large-scale environmental parameters, such as the SST, sea level pressure, OLR, 850-hPa relative vorticity

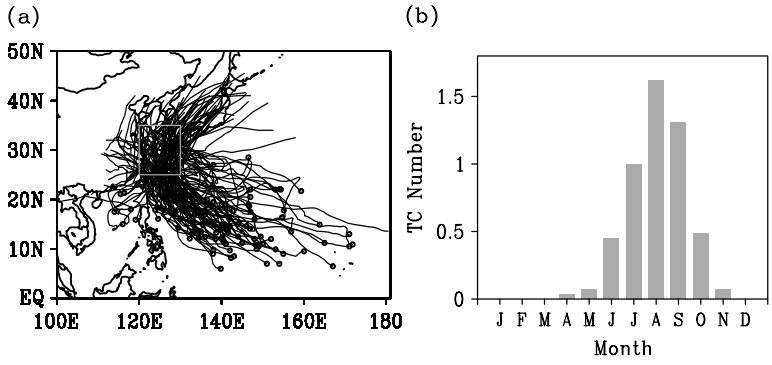

Figure 1. (a) Best tracks of tropical cyclones and (b) their monthly distribution over the East China Sea (25–35°N, 120–130°E) during 1979–2007. The box denotes the prediction target region.

and 850-hPa zonal wind (i.e. potential predictors) during the preceding months, for the first 25 years (1979–2003) of the analysis period. The last 4 years (2004–2007) are reserved as a period independent from the predictor analysis to check the availability of the predictors analysed in the earlier period. Among the environmental parameters, the SST and sea level pressure have large and consistent lag correlations from the preceding winter to spring (figure not shown). However, the other parameters lack consistency in the lag-correlation patterns during the preceding seasons. Physically interpretable signals for these parameters are found only in June. Considering the lag-correlation patterns and the physical meaning of the environmental parameters, we select the SST and sea level pressure averaged over the spring (March, April and May), along with the OLR, 850-hPa relative vorticity and 850-hPa zonal wind in June as potential predictors.

3.2.1. *Sea surface temperature*

Figure 2(a) shows the lagged correlation coefficients of the predictand with the SST over the Pacific Ocean in the preceding spring for 1979–2003. The light (dark) shading denotes the regions with a significantly positive (negative) correlation at the 95% confidence level. Variations of the SST over the remote ocean basin (i.e. central to eastern Pacific) rather than the WNP are found to have a larger lag-correlation on the seasonal TC frequency over the East China Sea. Because the SST over the western Pacific is high enough for developing TC during the boreal summer (>28.5 °C), the relationship between TC activity in WNP and the local SST is usually weak (Chan and Liu, 2004; Chan, 2007). Meanwhile, the interannual variations of the SST over the remote ocean basin are larger compared with those over the western Pacific warm pool, so that the stronger circulation response to

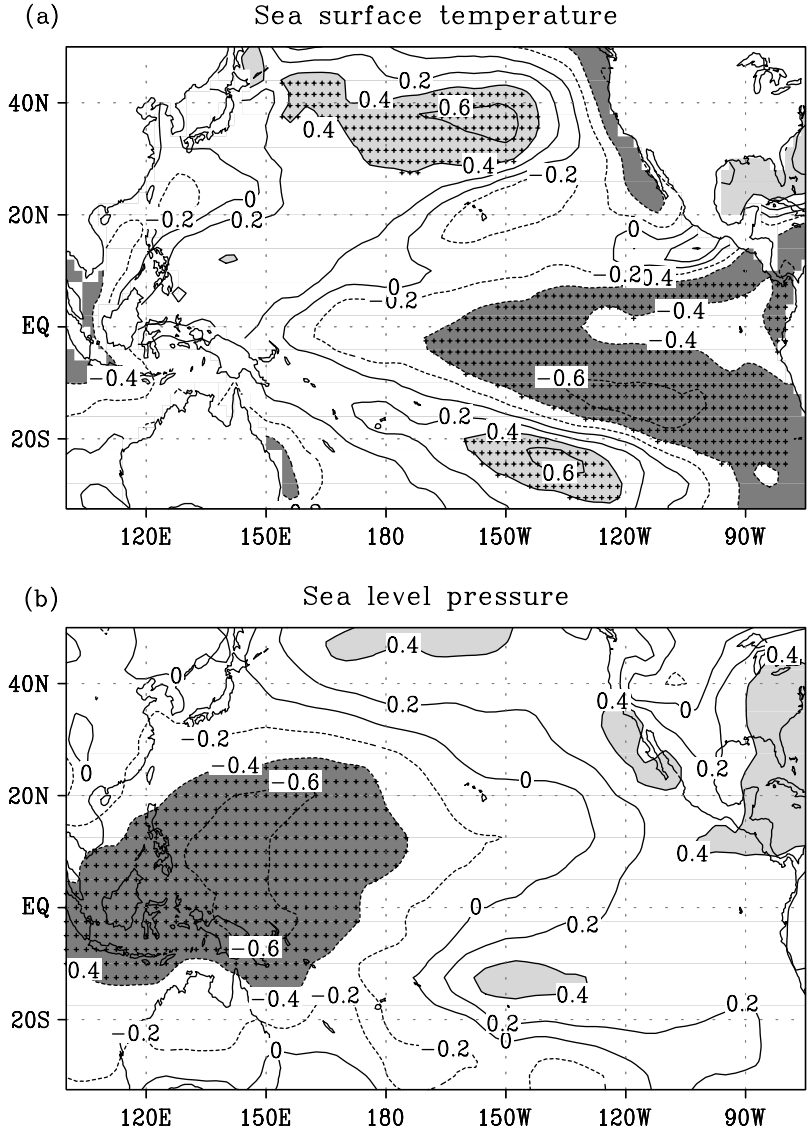

Figure 2. (a) The spatial distribution of lag-correlation coefficients between mean sea surface temperature for March to May and the number of tropical cyclones passing over the East China Sea for July to September. (b) Same as (a), except for mean sea level pressure. The light (dark) shading denotes the positively (negatively) correlated region at the 95% confidence level. The cross marks present the region selected as the potential predictors.

the remote SST can modify the dynamic parameters influencing TC genesis and the steering flows determining TC tracks.

While significant negative correlations exist over the tropical eastern Pacific, major positive correlations occur both north and south of it: one over the mid-latitude central North Pacific, and the other over the sub-tropical central South Pacific. The spatial distribution of the correlation coefficients may reflect the variability associated with ENSO (Harrison and Larkin, 1998). The correlation pattern persists from the preceding winter to spring and becomes weak during the peak TC season (figure not shown). It implies that the pre-season ENSO can be a precursory signal of the summer TC activity in the East China Sea. We examined the predictand for the boreal summers after the ENSO had a peak in pre-season. The ENSO events are selected when the Niño 3.4 index averaged for December–March exceeds one standard deviation. The TC frequencies in the summer after pre-season La Niña are 6 in 1985, 7 in 1989, 6 in 1999 and 6 in 2000, while those in the summer after pre-season El Niño are 1 in 1983, 4 in 1987, 3 in 1992, 3 in 1995, 2 in 1998 and 4 in 2003. This suggests that the pre-season La Niña (El Niño) may lead to higher (lower) TC frequency over the East China Sea during the summer. The pre-season ENSO affects the monsoon trough over the WNP (Wu and Wang, 2002) which may be responsible for the change in TC frequencies over the East China Sea in summer (Camargo *et al*., 2007).

Considering the lag-correlation pattern with the spring SST, the aforementioned three regions, that exhibit strong correlations with TC frequency over the East China Sea, are selected. The potential SST predictor is obtained as the sum of the average SST over two positively correlated regions, minus the average SST over the negatively correlated region for the preceding spring.

3.2.2. *Sea level pressure*

Figure 2(b) is the lagged correlation between TC frequency and the preceding spring sea level pressures. A broad area with significant negative correlation values is found in the tropical WNP. Just as in Figure 2(a), the correlation pattern mainly reflects the ENSO signal, the effects of which were discussed. This means that the anomalously low sea level pressure over the WNP may be a precursory signal for an abundance of TCs over the East China Sea during the summer. Therefore, the spring sea level pressure averaged over the tropical western Pacific, which is statistically significant at the 95% confidence level, was chosen as another potential predictor.

3.2.3. *Outgoing long-wave radiation*

The lagged correlation of the predictand with the antecedent OLR in June for the period 1979–2003 is shown in Figure 3(a). A negative correlation prevails throughout the tropical WNP, indicating that an active convection is conductive for TC occurrences over the East China Sea. The significant negative correlation values over the WNP imply that the OLR anomaly in June may persist in the following months (figures not shown), which affects TC activity in those months. Thus, we define a third potential predictor as the average OLR over the regions within 140–180 °E and 10–20°N where the negative correlation values are statistically significant at the 95% confidence level.

3.2.4. *850-hPa zonal wind*

Figure 3(b) is the lagged correlation between TC frequency and the 850-hPa zonal wind during the preceding June. The correlation pattern seems to represent a strong WNP summer monsoon (Wang *et al*., 2001), during which the monsoon trough extends further to the east and the easterlies prevail north of the monsoon trough, including the East China Sea. The monsoon trough variation is also related to the ENSO. As the SST over the NINO3.4 region is increased, the equatorial anomalous westerly over the WNP becomes stronger and the monsoon trough tends to extend eastward. The correlation

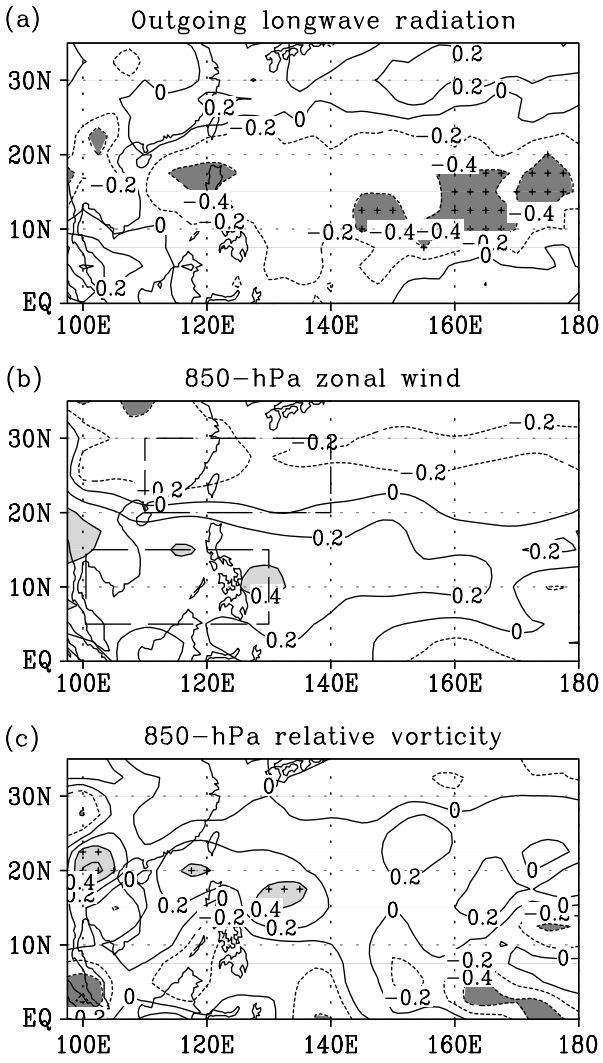

Figure 3. Same as in Figure 2, except for (a) the outgoing long-wave radiation in June, (b) the 850-hPa zonal wind in June and (c) the 850-hPa relative vorticity in June.

pattern becomes stronger in July–September (figure not shown). These large-scale environments may form more TCs over the Philippine Sea (Matsuura *et al*., 2003) and steer them to the East China Sea. Hence, we judiciously choose the WNP monsoon index as a fourth potential predictor. The WNP monsoon index is generally defined as the difference in the 850-hPa zonal winds between the entrance region (5–15°N, 100–130°E) and the outflow region (20–30°N, 110–140°E) (Wang *et al*., 2001). The correlation coefficient between the WNP monsoon index in June and the predictand is 0.41, which is significant at the 95% confidence level.

3.2.5. 850-hPa relative vorticity

Lastly, the lagged correlation with the 850-hPa relative vorticity in June is presented in Figure 3(c). The positively correlated regions are found along the latitude 20°N. The correlation pattern mainly reflects the WNP monsoon signal, the effects of which have already been mentioned. It implies that the positive vorticity anomaly in June tends to be followed by active summer TC activity over the East China Sea. Thus, the average 850-hPa relative vorticity, where the correlation coefficients are significant at the 95% confidence level (cross marked regions in Figure 3(c)), is chosen as a fifth potential predictor.

3.3. Predictor screening

The inclusion of many potential predictors in the multivariate regression model does not ensure better predictability, even if all of them are dynamically relevant predictors. Moreover, the five potential predictors analysed in the above section are mutually correlated because they are sensitive to large-scale circulation patterns such as the ENSO and the WNP monsoon. Blindly combining all of the predictors in a regression setting may lead to poor prediction (Wilks, 2006). Therefore, we attempted to select a best set of predictors from the pool of potential predictors by stepwise regression. In the stepwise regression, the regression is repeated by increasing the number of predictors starting from one, and the best set of predictors is determined by comparing the results of the regression at each step (Hastenrath *et al*., 1984).

The results of the stepwise regression using the LAD regression are presented in Table I. At each step, SAE, R^2 and the regression coefficient are checked while keeping in mind that a good predictor must have a lower SAE and a higher R^2. Besides, the regression coefficient must have the same sign, with a corresponding correlation coefficient, between the predictor and the predictand; that is, the SST, relative vorticity and zonal wind must have positive regression coefficients and the sea level pressure and OLR must have negative regression coefficients with the predictand. In the beginning, we perform the LAD regression with one predictor only. As a result, the SST is identified as the primary predictor because the SAE is the lowest and the correlation coefficient is the highest among the five potential predictors. In the second step, a two-predictor LAD regression is considered, including the SST as the key predictor. When the 850-hPa relative vorticity is utilized as an additional predictor, the SAE is the lowest and the R^2 is the highest. Thus, the 850-hPa relative vorticity is chosen as the second primary predictor, and is added to the set of predictors. In a same

Table I. Sum of absolute errors (SAE), R-square (R^2) and regression coefficients (a) in each stage of stepwise LAD regression..

		SST	Sea level pressure (SLP)	OLR	850-hPa zonal wind (U850)	850-hPa relative vorticity (VOR)
1st step	SAE	22.17	27.11	27.45	30.92	23.34
one predictor	R^2	0.53	0.36	0.37	0.17	0.52
	a	$a_{SST} = 1.23$	$a_{SLP} = -1.01$	$a_{OLR} = -0.95$	$a_{U850} = 0.89$	$a_{VOR} = 1.37$
2nd step	SAE		21.11	21.31	21.72	19.27
Two predictors	R^2		0.54	0.55	0.54	0.63
Including SST	a		$a_{SST} = 0.73$	$a_{SST} = 0.99$	$a_{SST} = 1.04$	$a_{SST} = 0.82$
			$a_{SLP} = 0.56^*$	$a_{OLR} = -0.32$	$a_{U850} = 0.30$	$a_{VOR} = 0.56$
3rd step	SAE		18.03	17.94	18.18	
Three predictors	R^2		0.65	0.66	0.64	
Including SST and VOR	a		$a_{SST} = 1.14$	$a_{SST} = 0.75$	$a_{SST} = 0.57$	
			$a_{VOR} = 1.00$	$a_{VOR} = 0.57$	$a_{VOR} = 1.22$	
			$a_{SLP} = 0.62^*$	$a_{OLR} = -0.12$	$a_{U850} = -0.54^*$	
4th step	SAE		17.78		17.45	
Four predictors	R^2		0.67		0.67	
Including SST, VOR and OLR	a		$a_{SST} = 0.92$		$a_{SST} = 0.54$	
			$a_{VOR} = 0.79$		$a_{VOR} = 1.23$	
			$a_{OLR} = -0.26$		$a_{OLR} = -0.02$	
			$a_{SLP} = 0.48^*$		$a_{U850} = -0.53^*$	

The asterisk (*) denotes that the regression coefficient has an inconsistency in the sign of a correlation coefficient between the predictor and the predictand.

manner, the OLR is also chosen as a good predictor in the third step.

However, the sea level pressure and 850-hPa zonal wind are excluded from the set of predictors because they show incoherent regression coefficients as the steps increase. The regression coefficients of sea level pressure in the second, third and fourth steps are positive, which is inconsistent with the correlation coefficient between the sea level pressure and the predictand. Also, the 850-hPa zonal wind is positively correlated with the predictand, but the regression coefficients are negative in the third and fourth steps. The predictors of the SST and sea level pressure have the same physical meaning as the ENSO. Also, both the 850-hPa zonal wind and the 850-hPa relative vorticity are related to the WNP monsoon. So they are highly correlated to each other [correlation (SST, sea level pressure) $= -0.91$ and correlation (vorticity, zonal wind) $= 0.78$]. As a result, after one of the mutually correlated predictors is added, the other is found to be redundant. The exclusion of predictors that have incoherent regression coefficients is an obvious choice for the stability and parsimony of the regression-based prediction model.

In addition, we have examined the stepwise regression based on the Poisson regression method. While not shown in the table, the result of the stepwise Poisson regression is similar to the stepwise LAD regression. It is noted that the three predictors selected by stepwise regression are also correlated to each other [correlation (SST, vorticity) $= 0.44$, correlation (vorticity, OLR) $= -0.68$, and correlation (OLR, SST) $= -0.59$]. All three correlation coefficients are statistically significant at the 95% significant level, but not higher than those with the redundant predictors. Independently, we examine the VIF, which is widely used for the measure of a multicollinearity in the predictor set. The VIF is defined as $\mathrm{VIF}_i = 1/(1 - {R_i}^2)$, where ${R_i}^2$ is the multiple coefficient of determination in a regression of the ith predictor on all other predictors. The VIFs for SST, the 850-hPa relative vorticity and the OLR are 1.56, 1.87 and 2.32, respectively. The VIFs do not exceed 5 which is regarded as the critical threshold for detecting the multicollinearity (Haan, 2002). So, the SST, the 850-hPa relative vorticity and the OLR are finally selected as the set of predictors for the statistical models to forecast the summer TC frequency over the East China Sea. Three predictors explicitly stand for the effect of ENSO and the WNP summer monsoon.

4. Results and validation

In order to validate the forecasting skill of the developed model, we use a leave-one-out cross-validation method for 1979–2003, i.e. the period used for the predictor analysis. Cross validation, the so-called Jack-knife method, is usually applied for testing a statistical prediction model to predict seasonal TC activity (Gray *et al*., 1992; Elsner and Schmertmann, 1993; Chan *et al*., 1998; Chu *et al*., 2007). The estimations for each year during 1979–2003 are computed by the prediction model, which is adjusted using the observations for the rest of the 24-year period, excluding the prediction year. For example, the prediction of the TC frequency in 1995 is obtained by using the predictors of 1995 and the regression coefficients calculated by regression analysis for the periods of 1979–1994 and 1996–2003. Likewise, the estimations for the other years are obtained in a similar way. Also we used the predictors analysed for 1979–2003 to adjust the predictions for 2004–2007, i.e. the period independent from the predictor analysis. The forecasting value for any year (Y) in 2004–2007 is computed using the regression coefficients and the constant via the LAD or Poisson regression model using data from 1979 to Y−1, along with the predictors for the prediction year (Y).

Figure 4 shows the time series of the cross-validation results for 1979–2003 and the prediction results for 2004–2007. The predicted time series tends to fluctuate in accordance with the actual observations, and there is no systematic bias. The skills of the models are accessed via the root mean square error (RMSE) method, the correlation between the observations and the predicted values, and the mean square skill score (MSSS) in Table II. The MSSS is defined as the ratio of the

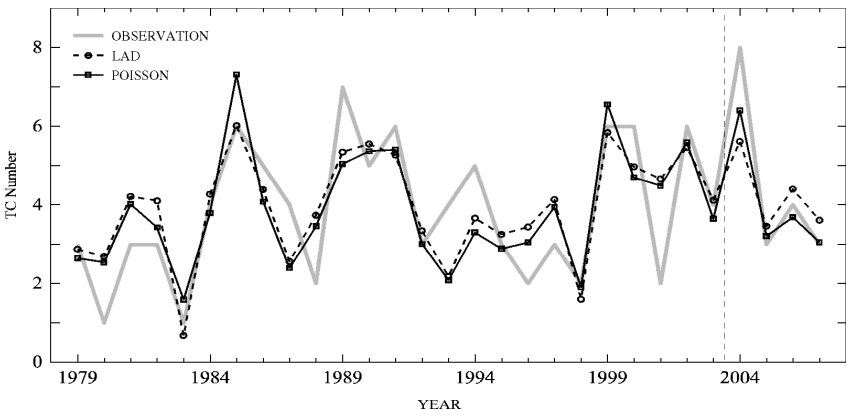

Figure 4. Time series of cross-validation results (1978–2003) and the prediction results (2003–2007) in the LAD model (dashed line) and the Poisson model (solid line), and the observed number of summertime tropical cyclones over the East China Sea (grey solid line).

Table II. The root mean square error (RMSE), the correlation coefficient and the mean square skill score (MSSS) of the LAD model and the Poisson model for 1979–2007.

	RMSE	Correlation	MSSS
LAD	1.15	0.75	0.60
Poisson	1.11	0.78	0.63

reduction in the mean square error of the predictions of the models compared to the reference forecasts based on the climatology value, which is recommended by the World Meteorological Organization (WMO) for the verification of deterministic seasonal forecasts (WMO, 2002). The RMSE is 1.15, the correlation coefficient is 0.75, and the MSSS is 0.60 for the LAD model, and are 1.11, 0.78 and 0.63, respectively, for the Poisson model. The correlation coefficients are significant at the 99.9% confidence level. Both models have a skill improvement of more than 60% over the reference forecast. The results suggest that both models are skillful in predicting summer TC frequency over the East China Sea. Especially, the Poisson model is slightly more skillful than the LAD model.

The prediction results for 2004–2007, which is a period independent from the predictor analysis, are shown in Table III. Both models fail to predict the extremely high number in 2004 (*cf*, Kim *et al*., 2005a) but are somewhat in line with the actual TC variation (Figure 4). The predictions of the Poisson model in 2005, 2006 and 2007 are closer to observations. The RMSE is 1.28 in the LAD model and 0.82 in the Poisson model. Overall, the RMSE values for the prediction period show comparable magnitude to those for the analysis period, indicating a reliable prediction skill.

To further examine the skill in predicting the seasonal TC activity over the East China Sea, we classify the TC counts into three categories, e.g. 'above normal (AN)', 'normal (N)' and 'below normal (BN)'. The average number of summer TCs passing over the East China Sea is about 4.0. So the years when the seasonal TC counts are 4 are defined as category N. The category AN (BN) is defined as those years when the seasonal TC counts are equal to or greater than 5 (equal to or less than 3). The results of the model are also divided by the same thresholds after the values are rounded off to integers. The results of the comparison between the observed

Table III. Seasonal predictions of TC frequency over the East China Sea using two methods.

	Observation	LAD	Poisson
2004	8	5.6 (−2.4)	6.4 (−1.6)
2005	3	3.5 (+0.5)	3.2 (+0.2)
2006	4	4.4 (+0.4)	3.7 (−0.3)
2007	3	3.6 (+0.6)	3.1 (+0.1)
RMSE		1.28	0.82

Table IV. Contingency table between the observed TC frequency over the East China Sea and results of the LAD model (upper table) and the Poisson model (lower table).

		Observation			
		BN	N	AN	Total
LAD	BN	8	2	0	10
	N	5	3	2	10
	AN	1	0	8	9
	Total	14	5	10	29

		Observation			
		BN	N	AN	Total
Poisson	BN	11	2	1	14
	N	3	3	1	7
	AN	0	0	8	8
	Total	14	5	10	29

and the predicted categories are shown in Table IV. The diagonal values represent successful predictions and the others denote prediction failures. The results show that the LAD model correctly predicts 57% of category BN, 60% of category N and 80% of category AN. The Poisson model has similar results in the N and AN categories, and predict 78% in BN category.

The prediction skills for the categorical forecasts can be assessed using the Gerrity skill score (Gerrity, 1992), which is one of the skill scores recommended by the WMO for the evaluation of forecasts (WMO, 2002). The Gerrity skill score is defined as

$$\text{Gerrity skill score} = \sum_{i=1}^{3} p_{ij} s_{ij} \tag{5}$$

where p_{ij} are the ratios of the number in each cell to the total number. The s_{ij} are given by

$$s_{ij} = \begin{cases} \frac{1}{2}\left(\sum_{r=1}^{i-1} a_r{}^{-1} + \sum_{r=i}^{2} a_r\right), & i = j \\ \frac{1}{2}\left[\sum_{r=1}^{i-1} a_r{}^{-1} - (j-i) + \sum_{r=j}^{2} a_r\right], & i < j \\ \frac{1}{2}\left[\sum_{r=1}^{j-1} a_r{}^{-1} - (i-j) + \sum_{r=i}^{2} a_r\right], & i > j \end{cases} \tag{6}$$

$$a_r = \frac{1 - \sum_{r=1}^{i} p_r}{\sum_{r=1}^{i} p_r} \tag{7}$$

where p_r are the ratios of the number in each category of the observation to the total number. A Gerrity skill score of one represents a perfect forecast, zero is the same as the reference forecasts based on the climatology, and it

is negative if the forecasts are worse than the reference forecasts. The Gerrity skill scores of the contingency tables are 0.593 in the LAD model and 0.693 in the Poisson model. Thus the prediction skills of the models are higher than the reference forecasts. Moreover, the results show that the Poisson model is more successful in the prediction of regional TC frequency than the LAD model.

The mean regression coefficients and regression constants used in the LAD model and the Poisson model are shown in Figure 5. The error bars denote the standard deviation. All of them have small variations and show the same signs as the correlation coefficient between the predictor and the predictand, suggesting that the two models that were developed using the three predictors have stability and consistency in the process of prediction. The magnitudes of the regression coefficients imply the weights of each predictor in the prediction model because all the predictors are normalized. The SST appears to be a key predictor than the others in the LAD model because the regression coefficients of the SST have the largest magnitude among all three predictors. In the Poisson model, the contributions of the 850-hPa relative vorticity and SST are comparable. The OLR is a minor predictor in both the LAD and Poisson models. It is noted that the absolute value of the regression coefficients does not mean how much the predictors actually contribute to the TC variability over the East China Sea because the predictors are not completely independent from each other.

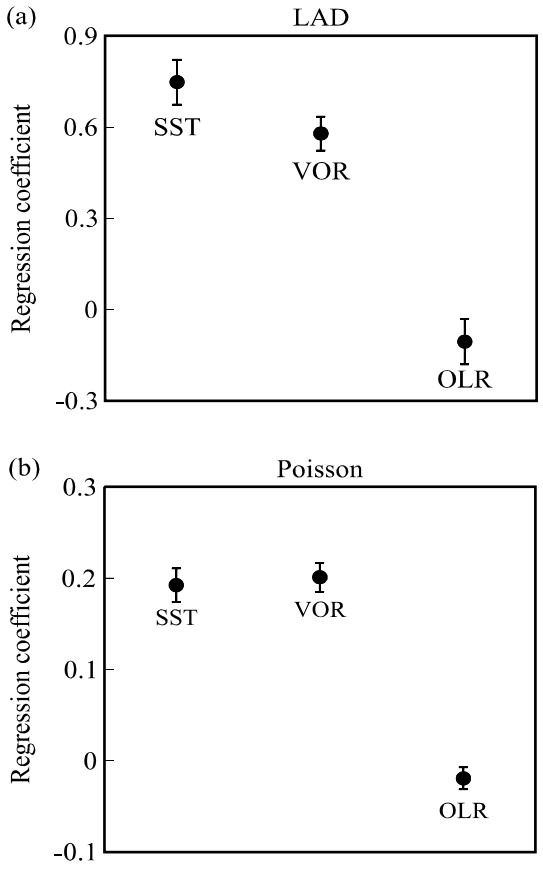

Figure 5. The average of the regression coefficients used in the LAD model and the Poisson model for 1979–2007. The error bars denote the standard deviation of each component.

5. Conclusion

Statistical models to predict the seasonal TC frequency over the East China Sea have been employed in the present study. The TCs passing over the East China Sea have the potential to affect East Asian countries where a large number of people live. The prediction season is confined to the summertime (July–September) because the number of TCs traversing the target region during this season exceeds 75% of the annual number and most of the damage caused by TCs in East Asia occurs during this time. The method applied to the statistical prediction models was based on the LAD regression and the Poisson regression, which have been known to be more appropriate in predicting seasonal TC activity.

The antecedent large-scale environmental parameters related to the summer TC frequency over the East China Sea, i.e. predictand, were analysed for the period of 1979–2003. The lag-correlation patterns of the predictand with the antecedent spring SST and sea level pressure showed ENSO-related patterns and those with the 850-hPa relative vorticity and 850-hPa zonal wind in June have the signal related to the WNP summer monsoon. The OLR in June also has significant signals related to the convective activity over the tropical WNP basin. Using the stepwise regression, the initial five potential predictors were screened to the final three predictors, i.e. the SST, 850-hPa relative vorticity and OLR. The SST was the combination of the SSTs in the three significantly correlated regions over the Pacific. The 850-hPa relative vorticity was averaged for a significant positively correlated region near the latitude of 20°N over the WNP and the OLR was averaged for a significant negatively correlated region over the tropical WNP.

We performed leave-one-out cross validation using the three predictors for 1979–2003 and the predictions for 2004–2006. The correlation coefficient between the estimations of the model and observations was 0.75 for the LAD model and 0.78 for the Poisson model. The RMSE is about 1.1 in both models. The models showed a seasonal prediction skill improvement of more than 60% compared with the reference forecasts. To evaluate the seasonal TC activity prediction, the TC counts were classified into three categories (i.e. BN, N and AN). While the models exhibited comparable skill in forecasting the above and near normal TC frequencies, the performance of the LAD model was slightly inferior to the Poisson model in the BN category. The regression coefficients and constants of the models showed stability and consistency during the prediction process. These results imply that both the LAD model and the Poisson model are skillful in predicting the summer TC frequency over the East China Sea, and that the Poisson model slightly outperforms the LAD model.

In this study, only the reasonably relevant large-scale environmental parameters were selected as predictors. In this regard, the forecasts were not due to random chance but are supported by plausible physical mechanisms instrumental for TC occurrences. Meanwhile, this research suggests that seasonal TC activity over a regional domain, such as the East China Sea, can be skillfully predicted using lag-correlated large-scale environmental parameters. The methodology of this work can be applied to the prediction of TC activity over another region. It is anticipated that the present research will be helpful to forecasters in other TC-prone countries.

Acknowledgements

This work was funded by the Korea Meteorological Administration Research and Development Program under grant CATER 2006-4204. Hyeong-Seog Kim was supported by the BK21 project of the Korean government. The authors sincerely thank the anonymous reviewer for the valuable comments.

References

Bloomfield P, Steiger WL. 1980. Least absolute deviations curve-fitting. *Journal of Scientific and Statistical Computing* **1**: 290–301, DOI: 10.1137/0901019.

Camargo SJ, Robertson AW, Gaffney SJ, Smyth P, Ghil M. 2007. Cluster analysis of typhoon tracks. Part II: Large-scale circulation and ENSO. *Journal of Climate* **20**: 654–3676.

Chan JCL. 2007. Interannual variations of intense typhoon activity. *Tellus* **59A**: 455–460.

Chan JCL, Liu KS. 2004. Global warming and western North Pacific typhoon activity from an observational perspective. *Journal of Climate* **17**: 4590–4602, DOI: 10.1175/3240.1.

Chan JCL, Shi JE, Lam CM. 1998. Seasonal forecasting of tropical cyclone activity over the western North Pacific and the South China Sea. *Weather and Forecasting* **13**: 997–1004.

Chan JCL, Shi JE, Liu KS. 2001. Improvements in the seasonal forecasting of tropical cyclone activity over the western North Pacific. *Weather and Forecasting* **16**: 491–498.

Chu PS. 2004. ENSO and tropical cyclone activity. In *Hurricanes and Typhoons: Past, Present, and Potential*, Murnane RJ, Liu KB (eds). Columbia University Press: New York; 297–332.

Chu PS, Zhao X, Lee CT, Lu MM. 2007. Climate prediction of tropical cyclone activity in the vicinity of Taiwan using the multivariate least absolute deviation regression method. *Terrestrial Atmospheric and Oceanic Sciences* **18**: 805–825, DOI: 10.3319/TAO.2007.18.4.805(A).

Elsner JB, Jagger TH. 2006. Prediction models for annual U.S. hurricane counts. *Journal of Climate* **19**: 2935–2952, DOI: 10.1175/JCLI3729.1.

Elsner JB, Schmertmann CP. 1993. Improving extended-range seasonal predictions of intense Atlantic Hurricane activity. *Weather and Forecasting* **8**: 345–351.

Gerrity JP Jr. 1992. A note on Gandin and Murphy's equitable skill score. *Monthly Weather Review* **120**: 2707–2712.

Gray WM, Landsea CW, Mielke PW, Berry KJ. 1992. Predicting Atlantic seasonal hurricane activity 6–11 months in advance. *Weather and Forecasting* **7**: 440–455.

Gray WM, Landsea CW, Mielke PW, Berry KJ. 1993. Predicting Atlantic basin seasonal tropical cyclone activity by 1 August. *Weather and Forecasting* **8**: 73–86.

Gray WM, Landsea CW, Mielke PW, Berry KJ. 1994. Predicting Atlantic basin seasonal tropical cyclone activity by 1 June. *Weather and Forecasting* **9**: 103–115.

Haan CT. 2002. *Statistical Methods in Hydrology*, 2nd edn. Iowa State University Press: Iowa; 378.

Harr PA, Elsberry RL. 1995. Large-scale circulation variability over the tropical western North Pacific. Part I: Spatial patterns and tropical cyclone characteristics. *Monthly Weather Review* **123**: 1225–1246.

Harrison DE, Larkin NK. 1998. El Nino-Southern Oscillation sea surface temperature and wind anomalies 1946–1993. *Reviews of Geophysics* **36**: 353–399.

Hastenrath S, Wu MC, Chu PS. 1984. Towards the monitoring and prediction of north-east Brazil droughts. *Quarterly Journal of the Royal Meteorological Society* **110**: 411–425, DOI: 10.1002/qj.49711046407.

Hess JC, Elsner JB, LaSeur NE. 1995. Improving seasonal hurricane predictions for the Atlantic basin. *Weather and Forecasting* **10**: 425–432.

Ho CH, Baik JJ, Kim JH, Gong DY, Sui CH. 2004. Interdecadal changes in summertime typhoon tracks. *Journal of Climate* **17**: 1767–1776.

Ho CH, Kim JH, Kim HS, Sui CH, Gong DY. 2005. Possible influence of the Antarctic Oscillation on tropical cyclone activity in the western North Pacific. *Journal of Geophysical Research* **110**: D19104, DOI:10.1029/2005JD005766.

Kanamitsu M, Ebisuzaki W, Woollen J, Yang SK, Hnilo J, Fiorino M, Potter GL. 2002. NCEP-DOE AMIP-2 reanalysis (R-2). *Bulletin of the American Meteorological Society* **83**: 1631–1643, DOI: 10.1175/BAMS-83-11-1631.

Kim JH, Ho CH, Sui CH. 2005a. Circulation features associated with the record-breaking typhoon landfall on Japan in 2004, Geophysical Research Letters. *Geophysical Research Letters* **32**: L114713, DOI:10.1029/2005GL022494.

Kim JH, Ho CH, Sui CH, Park SK. 2005b. Dipole structure of interannual variations in summertime tropical cyclone activity over East Asia. *Journal of Climate* **18**: 5344–5356.

Kim JH, Ho CH, Kim HS, Sui CH, Park SK. 2008. Systematic variation of summertime tropical cyclone activity in the western North Pacific in relation to the Madden-Julian oscillation. *Journal of Climate* **21**: 1171–1191.

Kwon HJ, Lee WJ, Won SH, Cha EJ. 2007. Statistical ensemble prediction of the tropical cyclone activity over the western North Pacific. *Geophysical Research Letters* **34**: L24805, DOI:10.1029/2007GL032308.

Lee WJ, Park JS, Kwon HJ. 2007. A statistical model for prediction of the tropical cyclone activity over the western North Pacific. *Journal of the Korean Meteorological Society* **43**: 175–183.

Liu KS, Chan JCL. 2003. Climatological characteristics and seasonal forecasting of tropical cyclones making landfall along the South China coast. *Monthly Weather Review* **131**: 1650–1662, DOI: 10.1175//2554.1.

McDonnell KA, Holbrook NJ. 2004. A Poisson regression model of tropical cyclogenesis for the Australian Southwest Pacific Ocean region. *Weather and Forecasting* **19**: 440–455.

Matsuura T, Yumoto M, Iizuka S. 2003. A mechanism of interdecadal variability of tropical cyclone activity over the western North Pacific. *Climate Dynamics* **21**: 105–117.

Nakazawa T. 2006. Madden-Julian oscillation activity and typhoon landfall on Japan in 2004. *Science Online Letters on the Atmosphere* **2**: 136–139, DOI: 10.2151/sola.2006-035.

Saunders MA, Lea AS. 2005. Seasonal prediction of hurricane activity reaching the coast of the United States. *Nature* **434**: 1005–1008, DOI:10.1038/nature03454.

Wang B, Chan JCL. 2002. How strong ENSO events affect tropical storm activity over the western North Pacific. *Journal of Climate* **15**: 1643–1658.

Wang B, Wu R, Lau KM. 2001. Interannual variability of Asian summer monsoon: Contrast between the Indian and western North Pacific-East Asian monsoons. *Journal of Climate* **14**: 4073–4090.

Wilks DS. 2006. *Statistical Methods in the Atmospheric Science*, 2nd edn. Academic Press: London.

WMO. 2002. *Standardized Verification System for Long-range Forecasts, New Attachment II-9 to the Manual on the GDPFS (WMO-No. 485)*. World Meteorological Organization: Geneva.

Wu R, Wang B. 2002. A Contrast of the East Asian Summer Monsoon–ENSO Relationship between 1962–77 and 1978–93. *Journal of Climate* **15**: 3266–3278.

